Skin Contact Force Information in Sensory Nerve Signals Recorded by Implanted Cuff Electrodes

Morten K. Haugland, J. Andy Hoffer, and Thomas Sinkjaer

Abstract—When functional neuromuscular stimulation (FNS) is used to restore the use of paralyzed limbs after a spinal cord injury or stroke, it may be possible to control the stimulation using feedback information relayed by natural sensors in the skin. In this study we tested the hypothesis that the force applied on glabrous skin can be extracted from the electroneurographic (ENG) signal recorded from the sensory nerve. We used the central footpad of the cat hindlimb as a model of the human fingertip and recorded sensory activity with a cuff electrode chronically implanted around the tibial nerve. Our results showed that the tibial ENG signal, suitably filtered, rectified, and smoothed carries detailed static and dynamic information related to the force applied on the footpad. We derived a mathematical model of the force-ENG relation that provided accurate estimates of the ENG signal for a wide range of force profiles, amplitudes, and frequencies. Once fitted to data obtained in one recording session, the model could be made to fit data obtained in other sessions from the same cat, as well as from other cats, by simply adjusting its overall gain and offset. However, the model was noninvertible; i.e., the force could not be similarly predicted from the ENG signal, unless additional assumptions or restrictions were introduced. We discuss the reasons for these findings and their implications on the potential use of nerve signals as a source of continuous force feedback information suitable for closed-loop control of FNS.

I. INTRODUCTION

WHEN functional neuromuscular stimulation (FNS) is used to restore the use of paralyzed muscles, the forces generated depend in complex ways on the stimulation intensity, length of the muscle, recent activation history (e.g., muscle fatigue), type and placement of the stimulation electrode(s), and type of muscle. Some of these problems could be overcome if feedback information about the actual forces produced were available. Feedback may also be used to make corrections if the movement is disturbed externally, or if the parameters of the muscle(s) change (e.g., Crago et al. [2]).

With the advent of fully implantable open-loop stimulation systems (Donaldson [4], Smith et al. [31], Peckham and Keith [47]), it is realistic to also consider implanting closed-loop

M. K. Haugland and T. Sinkjaer are with the Department of Medical Informatics and Image Analysis, Institute of Electronic Systems, Aalborg University, DK 9220 Aalborg, Denmark.

J. A. Hoffer is with the School of Kinesiology, Faculty of Applied Sciences, Simon Fraser University, Burnaby, B.C., V5A 1S6, Canada.

IEEE Log Number 9401401.

systems, once reliable sensors become available. Implanted sensors can in principle overcome the typical shortcomings of external sensors that have made the latter impractical beyond the laboratory (cumbersome installation, calibration drift, sensitivity to ambient moisture and temperature, bulky size, cosmetically unacceptable appearance; reviewed by Benotas et al. [42]; Webster [38]). In the intact organism, natural sensors relay information about a multitude of variables such as pressure, joint angle, muscle force, or length (reviewed by Mountcastle [22], Burgess and Perl [1], Hensel [10], Skoglund [30], Vallbo et al. [37], Willis and Coggeshall [40]).

The present study addressed the hypothesis that the electrical activity of sensory nerve axons that innervate skin mechanoreceptors is closely related to the force applied on glabrous skin. It should be possible to record sensory nerve activity even if patients no longer have direct conscious sensation, because central lesions usually do not affect limb mechanoreceptors or their afferent nerve fibers (Thomas and Westling [33]). Tactile mechanoreceptors in the human hand relay detailed information about local deformations and forces that occur at the glabrous skin of the fingertips (Phillips et al. [23], Schmidt et al. [27], Srinivasan et al. [32]). The activity patterns of tactile mechanoreceptors have been studied in awake volunteers using microneurography (Vallbo and Hagbarth [36]). Four types of low-threshold mechanoreceptors with myelinated (Aδ) fibers (SA I, SA II, FA I, and FA II) have been identified in human glabrous skin (reviewed by Vallbo and Johansson [37]) that differ in their receptive field properties and discharge in response to standardized mechanical input to the skin (Knibestöl and Vallbo [19]), and during precision grip tasks (Westling and Johansson [39]). The dynamic sensitivity of most glabrous skin mechanoreceptors is highest at low grip forces, when the change in skin indentation to a fixed change in force is relatively greater (Westling and Johansson [39]; see also Pubols [25]).

We used the central footpad of the cat hindlimb as a model of glabrous skin in human fingertips. Single-unit studies have shown strong similarities between glabrous skin receptors in the cat footpad and in primates. With the exception of receptors with SA II properties, which are rarely found in the cat, receptors with similar physiological and morphological properties to human mechanoreceptors have been identified in the cat footpad (Lynn [45], Jänig [44], Burgess and Perl [1], Iggo and Ogawa [43]): SA units (comparable to human SA I units), RA units (comparable to human FA I units), and PC units (comparable to human FA II units). The innervation densities are somewhat lower in the cat footpad; in the

human fingertip there are about 240 units/cm^2 (Johansson and Vallbo [46]), whereas the central footpad of the cat contains about 300 units (Jänig [44]; area of footpad about 2 cm^2). Perpendicular application of forces that were in the range of naturally occurring forces during quiet standing produced skin indentations that were sufficient to exceed the threshold of most mechanoreceptors.

If a clinically applicable approach for closed-loop control is to be developed, the source of feedback signals should be invariant over time. By using whole-nerve cuff electrodes, the present study was aimed at monitoring the summed activity of all the axons that innervate an area of skin. This avoided the problems of specificity of location of the skin stimulus, and drift and fragility of electrodes that record from only a small number of axons (Hoffer [11], Hoffer and Haugland [15]). Whole-nerve cuff electrodes are robust, have been shown to record stable invariant electroneurographic (ENG) signals over extended periods of time (months and years), and have a solid record of long-term safety and stability when correctly designed, constructed, and installed (reviewed by Glenn and Phelps [5], Hambrecht and Reswick [7], McNeal and Bowman [20], Hoffer [11]). The nerve cuff signal reflected both the recruitment of mechanoreceptors and changes in the firing patterns of active receptors responding to the changing mechanical stimulus.

Preliminary results of this study have been reported (Hoffer et al. [13], [14], Sinkjaer et al. [28], Hoffer and Haugland [15]).

II. METHODS

The central footpad of the cat hindlimb served as our model of human glabrous skin. Ten adult male cats were purchased through the University of Calgary Animal Resources Center, individually housed in large dog cages (1×0.8×0.8 m), and maintained in accordance to the guidelines of the National Institutes of Health (USA) and the Canadian Council for Animal Care. Using aseptic techniques, a tripolar nerve recording cuff (reviewed by Hoffer [11]) was implanted on the tibial nerve, below the last motor branches that innervate calf muscles. The axons contained in the cuff were mainly sensory and innervated the plantar surface of the foot, including the footpads. The cuff was 3 or 4 cm long, had an inner diameter of 2.2 mm, and was implanted 2–4 cm above the ankle joint (see Fig. 1).

In four of the cats, a nerve blocking cuff was implanted on the tibial nerve proximal to the recording cuff, and a second recording cuff was placed on the sciatic nerve to make it possible to verify the block on the nerve by stimulating at one cuff and recording the compound action potential (CAP) at the other (Hoffer [11]). A venous catheter (a length of flexible silicone tubing, 1-mm inner diameter × 2-mm outer diameter) was implanted in a superficial jugular vein and emerged percutaneously at the back of the cat. This catheter allowed easy injection of fast-acting antibiotics and anesthetics. The leads from the chronically implanted electrodes emerged in the dorsolumbar region and were connected to a 40-pin connector sutured to the back of the cat (Hoffer [11]). To allow the
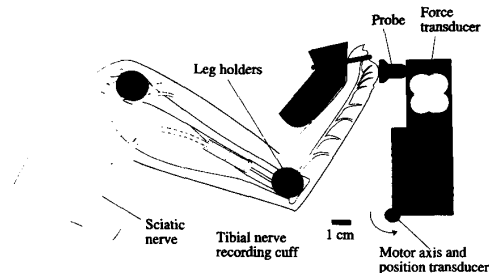

Fig. 1. Implanted nerve cuff location and experimental setup. The leg of the anaesthetized cat was fixed at the ankle malleoli and knee with atraumatic cupped clamps. The toes were fixed in a dorsiflexed position against a block by a string. Forces were produced by a controlled motor. ENG activity in the tibial nerve was recorded with a tripolar nerve cuff electrode.

devices to stabilize within the leg, the first experiments were performed 3–7 days after the implantation.

For recording experiments, the cats were initially anesthetized with Thiopentothal I.V. (8–10 mg/kg) through the implanted catheter, intubated with an intratracheal cannula, and deeply anaesthetized with Halothane in oxygen/nitrous oxide gas mixture. To reduce contribution from hair receptors in the skin to the overall activity recorded by the nerve cuff, the entire foot was shaved prior to each recording session and the remaining hair was removed with depilatory cream, followed by a thorough wash and application of moisturizing cream. The implanted leg was then mounted in a holder that consisted of 2 pairs of cupped clamps (see Fig. 1). One pair was secured around the ankle malleoli and the other around the knee, holding the leg in place without causing noticeable damage to the skin. A thick polyester suture loop held the toes in a dorsiflexed position, allowing the probe to touch the central footpad without involving the toes. This was also the natural position of the toes when the cat stood. The foot was kept warm with a heat lamp and the body and leg were wrapped in a heating pad, keeping the leg temperature around 34° C. A higher temperature in the leg (37–38° C) was difficult to keep stable, since the heating pad could not be allowed to touch the foot and since the heat lamp generated too much noise when close the leg. The design of the atraumatic leg holder allowed to carry out a series of recording sessions from each cat, repeated on average once per week.

Forces were applied to the footpad by a probe made of hard rubber with a flat smooth circular surface (diameter = 14 mm). The probe was attached to a printed motor with low inertia (PMI JR164CH) that was servocontrolled by a switching amplifier (PMI SSA-75-10-30) with velocity feedback combined with a variable amount of position and/or force feedback, giving a continuous range of stiffnesses from 100% stiff (strictly position feedback) to 100% compliant (strictly force feedback). It made in principle no difference what kind of feedback was used, but because the skin compliance was nonlinear (see Section III, Results) and since we wished to monitor the skin contact force for feedback purposes, most of the recordings were made with force feedback (see Pubols [25] for discussion). The command signal to the servo was generated by an IBM PC/AT-compatible 80386

microcomputer, sent to the servo amplifier via an analog port. In addition to controlling the motor, the computer sampled the force, position, and ENG and saved the data on the hard disk. Consecutive runs were spaced at least 10 s apart to allow receptors and skin to approach steady state.

The nerve signal was amplified with a low-noise preamplifier (QT 5-B, Leaf Electronics) at a gain of 1000. It was further amplified and bandpass filtered between 500 Hz and 10 kHz with a general purpose ac amplifier (Bak Electronics) and filtered through a third-order high-pass analog filter set at 1 kHz (Ithaco). Because the raw ENG had most energy in the range from 1 to 3 kHz (see Fig. 2(b)), sampling this signal directly would have required a fairly high sampling frequency. We assumed that the information about force, if present, would be in the 0–50-Hz range and would be available from the envelope of the ENG. Thus rectification and bin integration (RBI) of the raw ENG allowed us to reduce the sampling rate by sampling the envelope rather than the raw signal. The bin integrator (Bak PSI-1) worked by rectifying and integrating the neural signal into fixed duration bins (set in the range 1–10 ms), outputting the result from each integration through a sample-and-hold circuit (see Fig. 2(a)). To capture force transients in the 0–50-Hz range, the sampling frequency was set at 100 Hz and the bin duration for the integrator at 10 ms.

III. RESULTS

A. The Recorded Signal

When forces were applied to the central footpad of anesthetized cats, the ENG signal recorded from the tibial nerve was in the ±10-μV range (same as for conscious cats walking on a treadmill; Gordon et al. [6], Hoffer and Sinkjaer [12]). Fig. 2(a) shows an example of signals recorded during the present experiments. The top trace shows the force applied perpendicularly on the skin of the central footpad, in this case a step from zero to about 9 N that was held constant for 3.5 s and then returned to zero. The second trace shows the resulting indentation of the footpad, where zero corresponds to the probe just touching the uncompressed skin. The third trace shows the signal that was recorded from the tibial nerve cuff electrode, bandpass filtered between 1 kHz and 10 kHz, and sampled at 20 kHz. The bottom trace shows the ENG signal after rectification and bin-integration, sampled at 100 Hz. This corresponded to the envelope of the ENG signal and was assumed to be closely related to the overall firing frequency (aggregate activity) of the axons within the nerve cuff electrode.

The frequency content of the signal from the nerve cuff, filtered between 50 Hz and 10 kHz, is shown in Fig. 2(b). It verifies the findings of Gordon et al. [6], confirmed also by Milner et al. [21] for primate median nerve, that there is little neural energy below 1 kHz. Therefore, high-pass filtering at 1 kHz helped reduce noise pickup but did not remove significant information from the ENG signal.

During some of the experiments, lidocaine was infused in the blocking cuff to interrupt axonal conduction proximal
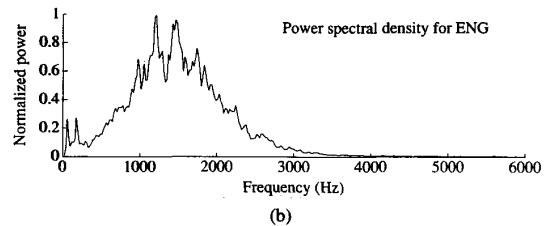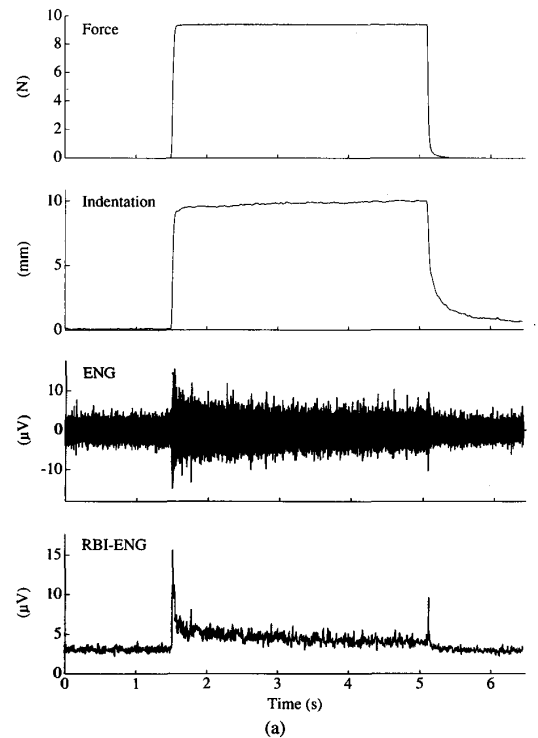

Fig. 2. (a) Top to bottom: Force, skin indentation, raw tibial ENG signal and rectified bin-integrated tibial ENG for a force step applied perpendicularly to the central footpad of anaesthetized cat 9. (b) Power spectral density of raw tibial ENG (bandpass filtered between 50 Hz and 10 kHz), calculated with a 1024-point FFT (fast Fourier transform) averaged over 3 s of data sampled at 20 kHz. The main energy in the signal is in the frequency range between 1 and 3 kHz. The nerve cuff electrode was 40 mm long.

to the recording cuff (viz., Hoffer [11]). No difference was apparent in the activity recorded from the nerve, confirming that it was purely of sensory origin and no significant spontaneous or reflex-mediated motor activity occurred during these experiments under anesthesia.

B. Properties of the ENG Versus Force

The cuff electrodes showed some activity at all times (see Fig. 2(a)), attributed partly to amplifier and thermal noise and partly to action potentials from receptors with resting firing rates different from zero. These sources contributed a constant level of activity for zero force, that rectification and filtering converted into a constant offset onto which the neural activity of interest was added.
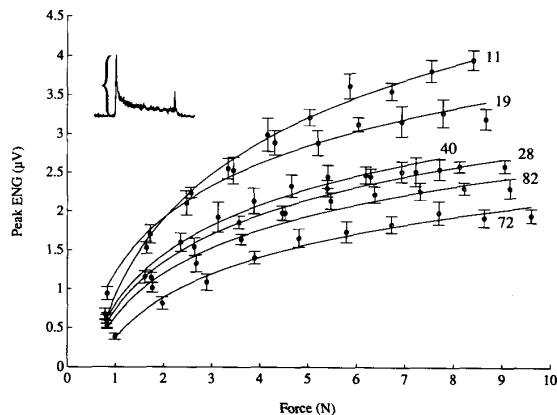
Fig. 3. Amplitude of the phasic RBI-ENG response as a function of force step size, measured with respect to background activity (inset). Each point is an average of 10 runs as the one in Fig. 2. Bars show ±1 SD. All graphs are from the same cat (#7) on different days, each labeled with the number of days since implantation. Fitted curves have the form: $K \log(S/S_0)$.

When a step force was applied on the skin, the ENG responded initially with a brief large peak and then decreased rapidly toward a new level. This level was higher than before the step onset, but continued to decrease slowly during maintained force. When the force step ended the ENG responded with a sharp peak of activity and then rapidly decreased to the same level as before force onset.

1) ENG Response to a Rapid Increase in Force: The amplitude of the ENG peak at force onset depended on the amplitude of the force step (Fig. 3). Each of the data points in Fig. 3 is the average of the peak amplitudes in 10 runs of the type shown in Fig. 2(a). Bars show ±1 standard deviation (SD). Peak values were defined from the smoothed ENG (11-point Hanning window), as the maximum voltage with respect to resting activity before the force was applied (see inset in Fig. 3).

The rate of rise of the force steps used in this series was the same for all step amplitudes (except maybe for the smallest steps, see Fig. 5(a)), to avoid any changes in peak ENG caused by this factor (see below). For the highest amplitude step, the rise time was less than 200 ms.

The amplitude of the ENG peak caused by the onset of a force step depended not only on the final amplitude of the force, but also on the rate of change of force. To show this dependency, ramp-and-hold forces with different ramp slopes were applied to the footpad. Twelve different slopes were applied, all of them rising to the same final of about 9 N (see Fig. 4(a)). The traces in Fig. 4 are averages of 10 runs for each ramp.

As could be expected, the ENG showed the strongest phasic response for the fastest rise in force. This dependency is shown in Fig. 4(b), where the amplitude of the first ENG peak is plotted against the rate of rise of the force. Each point in Fig. 4(b) is the average of 5 peak amplitudes at the same ramp velocity on the same day of recording (bars show ±1 SD) and different traces show data from different recording days for the same animal. Note the monotonic dependence of ENG peak amplitudes on the rate of rise of force, the low
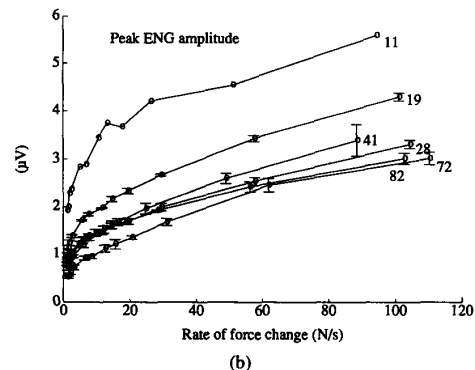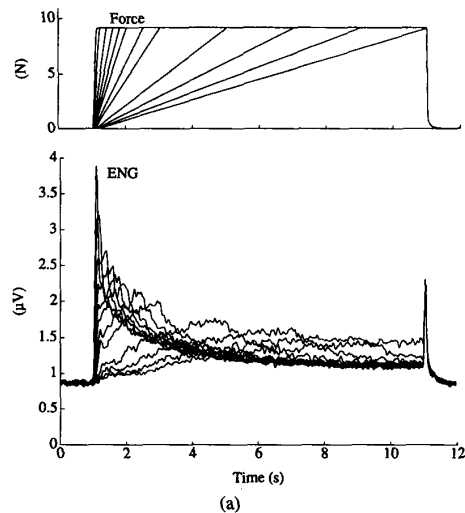

Fig. 4. (a) Ramp-and-hold forces applied on the footpad (top) and the corresponding tibial RBI-ENG signal (bottom). The amplitude of the initial phasic response increases with the rate of force increment. Notice also the very consistent off-response. (b) Peak ENG (relative to background activity) as function of force change rate. Each point is an average of 5, except for day 11, having only a single run per point. Bars show standard deviations. Data from cat 7 on different days of recording, as labeled.

intertrial variability, and different offset levels for different recording days. The day-to-day variability was attributed to gradual changes in cuff electrode impedance, overall gain, and/or variability in the position and angle of incidence of the test probe on the footpad (see Section V, Discussion).

The initial decay in ENG during maintained force steps of various amplitudes is shown in Fig. 5. Data are plotted in a double-logarithmic coordinate system to expand the display of the early phasic response. Note that the amplitude of the ENG peak scales with the amplitude of the force (as in Fig. 3) but in addition, the time of occurrence of the peak ENG is progressively delayed for larger amplitude force steps of similar rates of rise. The decay in ENG after the initial peak can be described by three linear segments when plotted in a log/log coordinate system (Fig. 5), indicating that the decay may be described as a sum of three power functions. This property was taken into consideration in developing a model of the ENG dependence on force (see below).
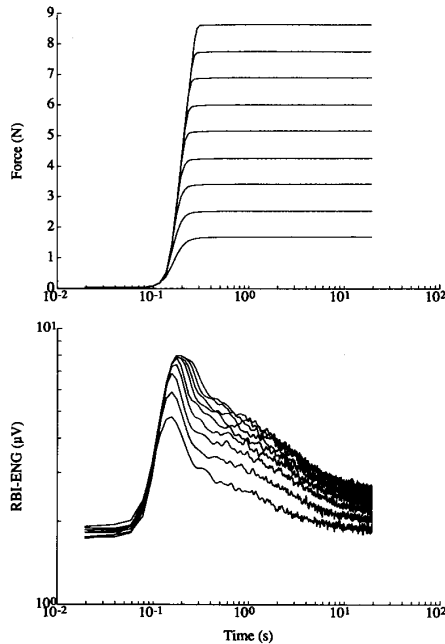
Fig. 5. Top: Force steps of increasing amplitude applied on footpad. Bottom: Corresponding RBI-ENG traces. Notice that the RBI-ENG peak amplitude at force onset was reached *before* the force had reached a steady state. In these log plots, the adapting RBI-ENG appears to consist of three linear segments, suggesting that the decay may consist of the sum of three power functions. Data from cat 9.
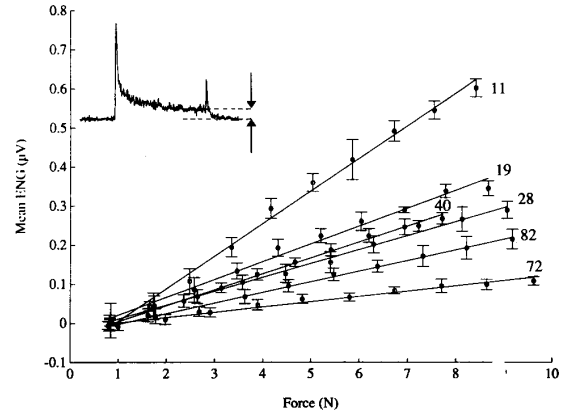

Fig. 6. Relation between steady-state force and RBI-ENG. The RBI-ENG amplitude was measured 15 s after force onset, relative to the RBI-ENG amplitude before the force was applied (inset). Each point is an average of 10 runs. Bars show ±1 SD. All graphs are from the same cat (#7), using data recorded on different postoperative days (as indicated). Notice the linear relation and the apparent threshold for detection of static forces at about 1 N.
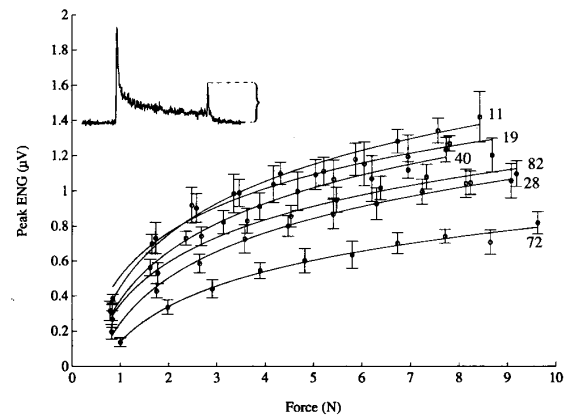

Fig. 7. Peak RBI-ENG amplitude at force removal (off-response) as a function of amplitude of force step. RBI-ENG amplitude was measured as shown in the inset. All graphs are from the same cat (#7) for different postoperative days. Fitted curves have the form: $K \log(S/S_0)$. Notice that they have similar shapes as the on-responses (Fig. 3) but lower amplitude.

Notice in Fig. 5 that the ENG reached its maximum value well before the force. This indicates that the peak ENG amplitudes plotted in Fig. 3 did not depend solely on force step amplitude, but rather reflected a combination of the rate of force rise and the duration of the rise. In Fig. 3 the ENG signals were smoothed with an 11-point Hanning window, resulting in smaller peak amplitudes for narrow peaks, whereas the ENG signals in Fig. 5 were smoothed with a Hanning window only 5 points wide. The smoothing was two-sided and had no effect on the position of the peaks in ENG.

2) ENG Activity During Maintained Force: When a force step was held constant for a prolonged period, the ENG approached a final value (Fig. 4(a)) that depended on the force step amplitude (Fig. 5). For each of the steps shown in Fig. 5, the mean ENG amplitudes measured 15 s after the onset of a force step are plotted in Fig. 6. A linear fit was usually obtained for data gathered on the same experimental day. The slope of the line fit, however, could change from day to day and from cat to cat. In Fig. 6, all of the fitted lines cross the horizontal axis at about 1 N, suggesting a threshold for the detection of static forces at that value. This was also the case for the other cats.

3) ENG Response to a Rapid Decrease in Force: When the force decreased rapidly towards zero, the ENG often showed a sharp positive peak. This behavior, referred to here as the "off-response," replicated observations of multiunit activity in human cutaneous nerves recorded with percutaneous microelectrodes (Vallbo and Hagbarth [36], Hulliger *et al.* [17]). For force changes that ended near zero,

the amplitude of the ENG peak depended on the magnitude of the force change (see Fig. 7) in a manner similar to the ENG peaks that occurred at force onset (shown in Fig. 3).

The ENG off-response was largest when the descending force step ended at a value close to zero. This is shown for a series of ascending and descending force steps in Fig. 8. The off-responses to the descending force steps were progressively larger, even though the force steps were of similar amplitude. The changes in skin indentation were considerably greater for fixed changes in force at low initial forces than for high ones, which probably accounted for the stronger off-responses at low forces.

C. Properties of the ENG versus Skin Indentation

The indentation (total perpendicular displacement of the skin surface from its undistorted position) was measured indirectly by a potentiometer coaxial with the printed motor,
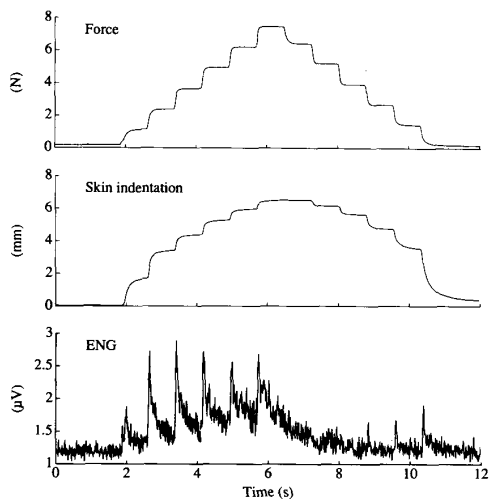
Fig. 8. Top: Staircase force applied to footpad. Middle: Skin indentation. Bottom: Rectified bin-integrated tibial RBI-ENG signal. Notice that the phasic response to similar decrements in force (off-response) increased as the force approached zero, as did the changes in skin indentation. Cat 5.

since the arm and force transducer were relatively stiff and the force was greater than zero in all cases (i.e., the probe did not lose contact with the skin). When a constant force was applied (see Fig. 2(a)) the indentation did not reach a constant level immediately after the rapid force onset; rather, it increased asymptotically towards a final value. Fig. 9(a) shows further that the force-indentation relation was not linear. The data shown in Fig. 9 are for several cycles of a 1-Hz sinusoidally varying force ranging from 0–8 N. Skin stiffness (the inverse of the slope) increased with indentation. This was attributed to the compression of soft tissues, as has been recognized for human skin by a number of investigators (see Westling and Johansson [39]). As was also the case for step inputs, there was significant settling of the skin, which caused a hysteresis loop; indentation changes lagged force changes. Also note that the indentation increased further for each turn in the loop, most significantly from the first time the force was increased to the next. This settling of skin was observed before (e.g., in sheep skin by Sakata *et al.* [26]). It was probably caused by slow changes in fluid perfusion through the tissue (Daly [3]).

The ENG responses can be described further by the changes in the skin indentation that accompanied the application of sinusoidally varying force. Fig. 9(b) shows the ENG response to 1-Hz sinusoidal forces applied to the footpad, as a function of force. Increases and decreases in the ENG signal led the increases and decreases in force, reflecting the dynamics of mechanoreceptors and giving rise to a large clockwise hysteresis loop. A smaller counterclockwise loop, apparent for low forces, was caused by the off-responses, i.e., by increases in ENG activity as the force declined toward zero. Fig. 9(c) shows the ENG as a function of the indentation. Here a large clockwise loop is also present, but the small loop is less apparent. This is partly because the off-responses occurred over a relatively larger range of indentation values, compared to the force. Notice also that the ENG response was largest during the first period of application of sinusoidal force. This
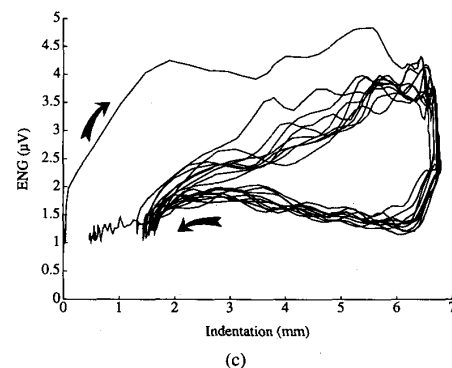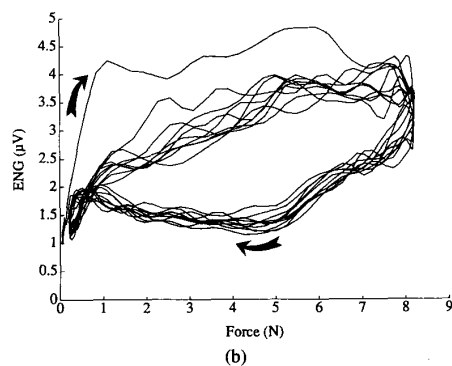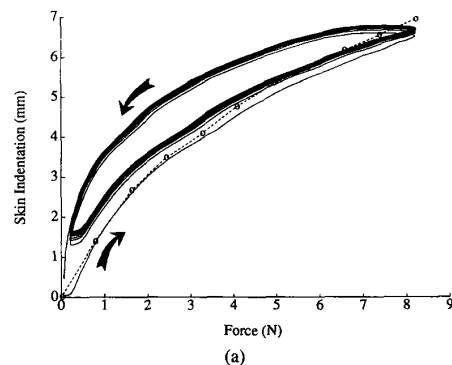

Fig. 9. Relation between skin contact force, skin indentation and RBI-ENG for a 1-Hz sinusoidal force for cat 6. (a) Indentation versus force. Dashed line is the relation for steady state (15 s after a step force onset). The relation is nonlinear, i.e., the footpad becomes less compressible for larger indentations, and for dynamic forces there is hysteresis, i.e., more force is required to reach a certain indentation when the force is increasing than when it is decreasing. (b) RBI-ENG versus force. (c) RBI-ENG versus indentation.

reflected the larger movement of the probe during the first period. In following periods, the skin indentation remained greater than zero by the time zero force was reached, because of the mechanical delay in the settling of the skin.

IV. MATHEMATICAL MODELING OF THE FORCE-TO-ENG RELATION

A. Construction of the Model

The purpose of this modeling effort was to describe the ENG signal in ways that would provide further information
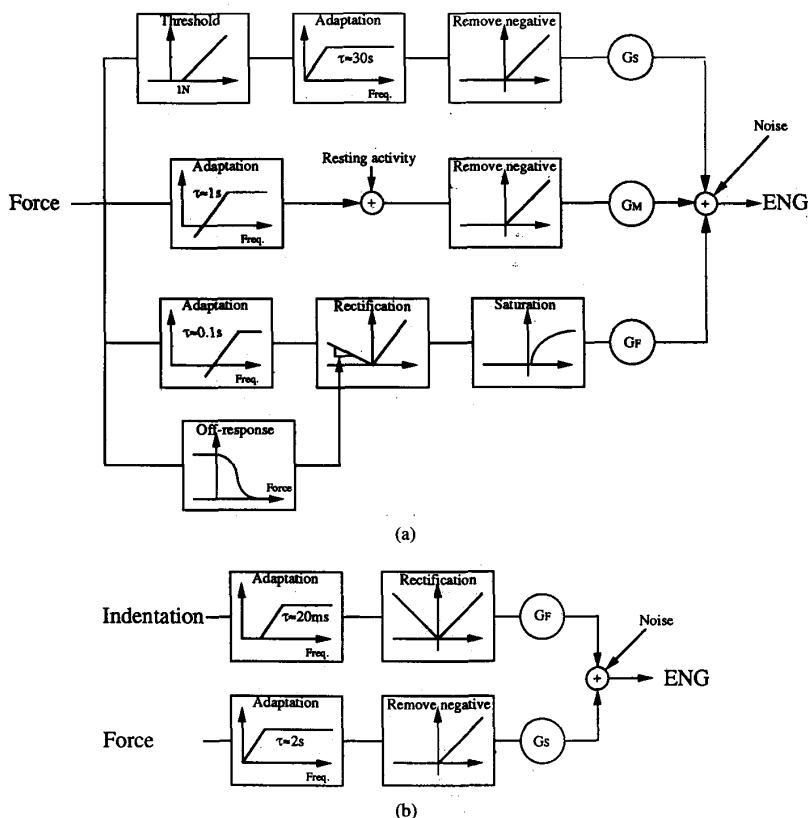
Fig. 10. (a) A three-compartment model of the RBI-ENG signal as a function of the force applied perpendicularly on the skin. (b) A two-compartment model of the RBI-ENG signal as function of the perpendicular force and the resulting indentation of the skin.

on the relevant skin inputs. Since perpendicular skin contact force was more interesting than skin indentation in the context of using ENG as a feedback signal for FNS, a model relating ENG to force was made first.

The three linear segments apparent in a log–log plot of the decay in ENG after a force step (Fig. 5(b)) suggest that the signal can be modeled as a sum of three power functions (Thorson and Biederman-Thorson [34]) or approximated by a sum of three exponential terms (Horch and Burgess [16]). Our model was constructed as a sum of three exponential components, each with a different rate of adaptation (slow, intermediate, and fast) and a different gain factor, as shown in Fig. 10(a). The adaptation for each component was modeled as a first-order high-pass filter, each with a different time constant. The output from each of the components was limited to positive values only, since neural activity could not have negative values.

The slow component was further equipped with an input threshold value, since there was no apparent response to constant forces lower than 1 N (viz., Fig. 6). Sometimes it was observed that after a descending step from high force to zero, the ENG level was initially lower than the resting level. The time course of return to the resting level was similar to the adaptation rate of the intermediate component and was thus

included by adding a constant level of activity (resting activity) to the intermediate component after the high-pass filter.

The most complex responses, however, were the off-responses that appeared when the force declined to a low or zero value. The time course of the off-response was similar to the fast component of the on-response, and the property was thus included in the fast component by adding a rectifying nonlinearity after the high-pass filter. An additional property of the off-response was that it depended not only on the change in force, but also on the level at which the change took place (e.g., Fig. 8). This property was modeled by changing the gain of the inverting slope of the rectifier as a function of the force. At forces close to zero the gain was high, and at high forces the gain was close to zero. The following sigmoid function was used:

$$G(\text{force}) = \frac{-K_{\text{off}}}{1 + \exp(Sl_{\text{off}}(\text{Force} - Th_{\text{off}}))}$$

where K_{off}, Sl_{off}, and Th_{off} are constants that determined the gain, slope, and threshold for the function and G is the gain of the inverting side of the rectifier.

The last part of the fast component was a static nonlinearity corresponding to the nonlinear slopes of the peak amplitude
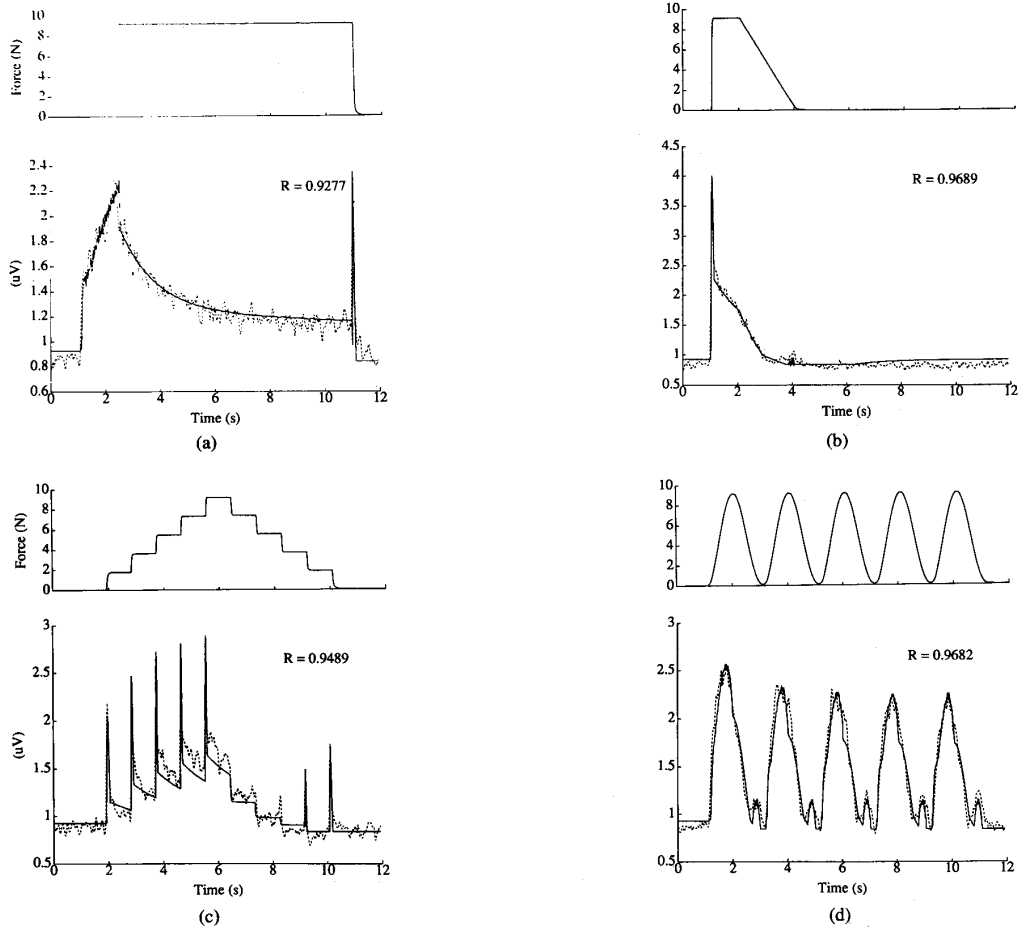
Fig. 11. Examples of predictions from the force-to-ENG model are compared with originally recorded RBI-ENG, for different force profiles (cat 7). Top trace is the force applied on the footpad and used as input to the model. Bottom dashed trace is the recorded RBI-ENG and the solid trace is the output of the model. (a), (b) Force profiles comparable to expected forces during precision grasp. (c) Test signal containing both tonic and phasic components to demonstrate the dependency on force of the off-response. (d) 0.5-Hz sinusoidal force profile, representing a more typical signal to test a dynamic model. All of these examples are different from the data files used for optimizing the parameters of the model.

of on- and off-responses shown in Fig. 3 and 7. This was modeled by the logarithmic function: $\log(S/S_0)$, where S is the input and S_0 the threshold value.

B. Model Performance

The parameters for the model were fitted with an automatic iterative procedure, the multidimensional downhill simplex method (Press *et al.* [24]) using as the initial guess a rough manual fit based on the parameter values described above. The algorithm minimized the mean squared difference between model output and recorded ENG (the error), using six representative data sets of force/ENG profiles. Six data sets were chosen so that they covered a wide range of frequencies and amplitude values in order to make the model perform as well as possible for any force profile. Fig. 11 shows comparisons of model output with the originally recorded ENG. It is important to note that the model parameters used in Fig. 11 were optimized using different data sets from the examples

shown in the figure, and that the parameter values were kept constant for all the trials in the figure.

The correlation coefficient between modeled and actual ENG was usually close to 0.95 and only in a few cases below 0.90. To obtain such a high level of predictive accuracy the model required adjustment of several parameters. In practice, several of the parameters could vary considerably without significantly changing the performance of the model. This was attributed to the fact that many parameters were dependent on others; i.e., it was difficult to find a unique parameter set that optimized the model. Importantly, when a set of parameters was found that optimized the model for one recording session, it was possible to accurately fit data from other sessions using the same parameters with the exception two: the noise level and a scaling factor. Table I shows a set of parameters found for cat 7 on day 82 after implant (*viz.*, Fig. 11). A model yielding practically the same performance for other recording sessions (with the same as well as other cats) could be made by changing the noise level and multiplying the summed output

TABLE I
PARAMETERS FOR THE FORCE-TO-ENG MODEL WHEN FITTED TO DATA OBTAINED FROM CAT 7 RECORDED ON DAY 82 AFTER IMPLANT

G_F (μV/V)	G_M (μV/V)	G_S (μV/V)	τ_F (ms)	τ_M (s)	τ_S (s)	S_0	Rest	K_{off}	Sl_{off}	Th_{off} (N)	Noise (μV)
0.46	0.12	0.04	15	1.3	29	0.03	0.7	0.97	1.2	1.6	0.84

TABLE II
SCALING FACTOR AND NOISE LEVEL ADJUSTMENTS REQUIRED TO
USE THE MODEL PARAMETERS FROM TABLE I TO FIT DATA
RECORDED ON OTHER DAYS FROM THE SAME OR DIFFERENT CATS

Cat	Day	Gain	Noise (μV)
5	48	2.41	1.62
5	53	1.33	1.19
6	20	2.21	1.11
6	27	1.98	1.07
7	11	2.32	1.86
7	19	1.55	1.24
7	28	1.24	0.72
7	40	1.36	0.85
7	82	1.00	0.84
9	12	3.57	2.01
11	0	1.24	3.47

from the three compartments with a constant, without changing any other parameter. Table II shows the noise level and scaling factors needed for the model parameters from Table I to also fit data from other recording sessions or other cats. Correlation coefficients ranged from 0.90 to 0.95.

It is observed in Table II that the scaling factors tended to be somewhat smaller over time, suggesting that nerve signals became smaller the longer the time the electrode had been implanted. Among several reasons which could explain this, one of concern was whether the nerve might have been chronically damaged by the cuff. However, none of the cats showed any signs of discomfort or of sensorimotor impairment. Since the noise level had a similar tendency to decline, it is more likely that the cause was the gradual decline in cuff electrode impedance that was typically recorded. For cat 7, for example, the impedance between the center cuff electrode and an implanted reference electrode declined from 3.1 kΩ to 2.4 kΩ between day 11 and day 82.

B. Model Based on Force and Indentation as Inputs

The model described above considered force as its only input, whereas the recorded signal reflected a combination of input force and skin indentation, which were not simply related to each other (Fig. 9). Also, the nonlinear dependence of off-responses to the absolute level of force as described above might be easier to model with indentation as an additional input. We therefore explored whether a simpler model could be constructed using force and indentation as two separate inputs. This took the form of a two-compartment model, shown in Fig. 10(b). The slow component took force as its input, since force and steady-state ENG activity were linearly related (Fig. 6). The rapidly adapting component took indentation as input, since the nonlinear force-indentation relation (Fig. 9(a)) could compensate for some of the nonlinear behavior of on- and off-responses (Figs. 3 and 7).

The new model (Fig. 10(b)) had only 5 parameters (gain and time constant for each compartment plus noise), compared to 12 parameters for the first model. The parameters were optimized as for the first model. The fits were less accurate in most cases, but still better than what could be obtained with a model of the same simplicity using only force as input (unpublished observations). The correlation coefficients were usually in the range 0.88–0.94.

V. DISCUSSION

This study has shown that ENG signals recorded from the cat tibial nerve with a cuff electrode contain reliable information about the force applied perpendicularly on the footpad. For any given input, the recorded ENG signal reflected the characteristic activity patterns of mechanoreceptors from glabrous skin (Vallbo and Johansson [37]) and also the skin deformation that caused varying numbers and types of units to respond to the applied force (Westling and Johansson [39], Pubols [25]).

The properties of the ENG signal were summarized in a model that was able to accurately estimate the nerve signal for different force inputs to the footpad. The model was robust for a large range of force profiles, amplitudes, and frequencies and was general enough to predict data obtained from the same cat on other days, or even from different cats, by simply recalculating two parameter values. A simpler model that used both force and skin indentation as inputs was found to perform almost as well as the more complex force-to-ENG model. This indicates that the complexity in the force-dependent model is indeed partly accounted for by the mechanical properties of the footpad.

We have earlier attempted to produce a force estimator based on the nerve signal, by using either analog nonlinear filtering (Hoffer et al. [13]), digital linear filter identification (Haugland [8]) as well as digital nonlinear optimization of a heuristic model (Haugland [8]) to produce a filter taking ENG as input and producing a force estimate as output based only on the properties of the force and ENG signals. These attempts produced good results for input forces within certain frequency ranges, but it was not possible to make a model that would compute acceptable estimates for wide ranges of force amplitudes and frequencies. The models presented here suggest that the reason for the earlier problem was that the relation from force to ENG is intrinsically nonlinear and noninvertible. The off-response property is especially problematic, since its rectifying nature partially removes information about the sign of a change in force (partially, because the off-response is present mainly for low forces). However, the model may still be invertible if there is also knowledge of expected force ranges and changes, based on the stimulation patterns dictated

by the FNS controller or information obtained from other sources. If so, this approach may prove sufficiently reliable for use in closed-loop control of FNS systems.

The basic features described for cat tibial nerves in this study were also present in human sural nerve recordings when comparable forces were applied on the skin of the dorsolateral foot (Haugland *et al.* [9]). Information recorded with a nerve cuff has already found application in an FNS system that did not require exact information about force amplitude, but rather about timing of skin loading. The ENG signal recorded with a cuff electrode implanted on the sural nerve of a hemiplegic human was used to accurately detect heel-to-floor contact and control a peroneal stimulation system for footdrop correction (Sinkjaer *et al.* [29]).

In order for cutaneous ENG signals to find general applications for the control of FNS in paralyzed humans, it is necessary to also demonstrate that reliable ENG signals can be recorded from peripheral nerves while nearby muscles are stimulated electrically. The problems of artifact pickup in nerve recordings are addressed in an accompanying paper (Haugland and Hoffer [41]).
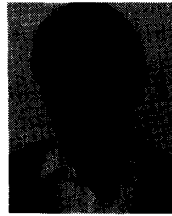
ACKNOWLEDGMENT

REFERENCES

[1] P. R. Burgess and E. R. Perl, "Cutaneous mechanoreceptors and nociceptors," in A. Iggo, Ed., *Handbook of Physiology, vol. II: Somatosensory System*, 1973, pp. 29–78.

[2] P. E. Crago, R. J. Nakai, and H. J. Chizeck, "Feedback regulation of hand grasp opening and contact force during stimulation of paralyzed muscle," *IEEE Trans. Biomed. Eng.*, vol. 38, pp. 17–28, 1991.

[3] C. H. Daly, "Biomechanical properties of dermis," *J. Investigative Dermatol.*, vol. 79, suppl. 1, pp. 17s–20s, 1982.

[4] N. de N. Donaldson, "A 24-output implantable stimulator for FES," in *Proc. 2nd Vienna Int. Workshop on Functional Electrostimulation*, 1986, pp. 197–200.

[5] W. W. L. Glenn and M. L. Phelps, "Diaphragm pacing by electrical stimulation of the phrenic nerve," *Neurosurgery*, vol. 17, pp. 974–984, 1985.

[6] T. Gordon, J. A. Hoffer, J. Jhamandas, and R. B. Stein, "Long term effects of axotomy on neural activity during cat locomotion," *J. Physiol.*, vol. 303, pp. 159–165, 1980.

[7] F. T. Hambrecht and J. B. Reswick, Eds., "Functional electrical stimulation: Applications in neural prostheses," *Biomed. Eng. Instrum. Ser. 3.* New York: Marcel Dekker, 1977.

[8] M. Haugland, "Natural sensory feedback in closed-loop control of paralyzed muscles," M.S. thesis, Aalborg University, 1989.

[9] M. Haugland, T. Sinkjaer, and J. Haase, "Force information in whole human sensory nerve recordings," in *Proc. 4th Vienna Int. Workshop on Functional Electrostimulation*, 1992, pp. 130–133.

[10] H. Hensel, "Cutaneous thermoreceptors," in A. Iggo, Ed., *Handbook of Sensory Physiology, vol. II: Somatosensory System*, 1973, pp. 79–110.

[11] J. A. Hoffer, "Techniques to study spinal-cord, peripheral nerve, and muscle activity in freely moving cats," *Neuromethods*, vol. 15, pp. 65–145, 1990.

[12] J. A. Hoffer and T. Sinkjaer, "A natural 'force sensor' suitable for closed-loop control of functional neuromuscular stimulation," in *Proc. 2nd Vienna Int. Workshop on Functional Electrostimulation*, 1986, pp. 47–50.

[13] J. A. Hoffer, M. Haugland, and T. Li, "Obtaining skin contact force information from implanted nerve cuff recording electrodes," in *Proc. 11th IEEE/EMBS Annu. Meeting*, Nov. 1989.

[14] J. A. Hoffer, M. Haugland, and T. Sinkjaer, "Functional restoration of precision grip using slip information obtained from peripheral nerve

[15] J. A. Hoffer and M. Haugland, "Signals from tactile sensors in glabrous skin suitable for restoring motor functions in paralyzed humans," in R. B. Stein, H. P. Peckham, and D. Popovic, Eds., *Neural Prostheses: Replacing Motor Function after Disease or Disability.* New York: Oxford Univ. Press, 1992, pp. 99–125.

[16] K. W. Horch and P. R. Burgess, "Long term adaptation of cutaneous type I and type II mechanoreceptors in the cat," *Chinese J. Physiol. Sci.*, vol. 1, pp. 54–62, 1985.

[17] M. Hulliger, E. Nordh, A-E. Thelin, and Å. B. Vallbo, "The responses of afferent fibres from the glabrous skin of the hand during voluntary finger movements in man," *J. Physiol.*, vol. 291, pp. 233–249, 1979.

[18] R. S. Johansson, "Tactile sensibility in the human hand: Receptive field characteristics of mechanosensitive units in the glabrous skin area," *J. Physiol.*, vol. 281, pp. 101–123, 1978.

[19] M. Knibestöl and Å. B. Vallbo, "Single unit analysis of mechanoreceptor activity from the human glabrous skin," *Acta Physiol. Scand.*, vol. 80, pp. 178–195, 1970.

[20] D. R. McNeal and B. R. Bowman, "Selective activation of muscles using peripheral nerve electrodes," *Med. Biol. Eng. Comput.*, vol. 23, pp. 249–253, 1985.

[21] T. E. Milner, C. Dugas, N. Picard, and A. Smith, "Cutaneous afferent activity in the median nerve during grasping in the primate," *Brain Res.*, vol. 548, pp. 228–241, 1991.

[22] V. B. Mountcastle, "Sensory receptors and neural encoding: introduction to sensory processes," in V. B. Mountcastle, Ed., *Medical Physiology*, vol. 1, 13th ed., 1974, pp. 285–306.

[23] J. R. Phillips, R. S. Johansson, and K. O. Johnson, "Representation of braille characters in human nerve fibers," *Exp. Brain Res.*, vol. 81, pp. 589–592, 1990.

[24] W. H. Press, B. P. Flannery, S. A. Teukolsky, and W. T. Vetterling, *Numerical Recipes in C, The Art of Scientific Computing.* New York: Cambridge Univ. Press, 1988.

[25] B. J. Pubols, Jr., "Slowly adapting Type I mechanoreceptor discharge as a function of dynamic force versus dynamic displacement of glabrous skin of raccoon and squirrel monkey hand," *Neurosci. Lett.*, vol. 110, pp. 86–90, 1990.

[26] K. Sakata, G. Parfitt, and K. L. Pinder, "Compressive behaviour of a physiological tissue," *Biorheology*, vol. 9, pp. 173–185, 1972.

[27] R. F. Schmidt, L. K. Wahren, and K.-E. Hagbarth, "Multiunit neural responses to strong finger pulp vibration. I. Relationship to age," *Acta Physiol. Scand.*, vol. 140, pp. 1–10, 1990.

[28] T. Sinkjaer, M. Haugland, J. Haase, and J. A. Hoffer, "Whole sensory nerve recordings in human—An application for neural prostheses," in *Proc. Annu. Int. Conf. IEEE EMBS*, vol. 13, pp. 900–901, 1991.

[29] T. Sinkjaer, M. Haugland, Haase, "The use of natural sensory nerve signals as an advanced heel-swithc in drop-foot patients," in *Proc. 4th Vienna Int. Workshop on Functional Electrostimulation*, Vienna, Austria, Sept. 24–27, 1992, pp. 134–137.

[30] S. Skoglund, "Joint receptors and kinaesthesis," in A. Iggo (Ed.), *Handbook of Physiology, Vol. II: Somatosensory System*, 1973, pp. 111–136.

[31] B. Smith, P. H. Peckham, M. W. Keith, and D. D. Roscoe, "An externally powered, multichannel, implantable stimulator for versatile control of paralyzed muscle," *IEEE Trans. Biomed. Eng.*, vol. 34, pp. 499–508, 1987.

[32] M. A. Srinivasan, J. M. Whitehouse, and R. H. LaMotte, "Tactile detection of slip: Surface microgeometry and peripheral neural codes," *J. Neurophysiol.*, vol. 63, pp. 1323–1332, 1990.

[33] C. K. Thomas and G. Westling, "Tactile afferent function after human cervical spinal cord injury," in *Proc. 22nd Annu. Meeting Soc. Neurosci.*, Anaheim, CA, 1992, p. 831.

[34] J. Thorson and M. Biederman-Thorson, "Distributed relaxation processes in sensory adaptation," *Science*, vol. 183, pp. 161–172, 1974.

[35] Å. B. Vallbo, K. E. Hagbarth, H. E. Torebjörk, and B. G. Wallin, "Somatosensory, proprioceptive, and sympathetic activity in human peripheral nerves," *Physiolog. Rev.*, vol. 59, 1979.

[36] Å. B. Vallbo and K.-E. Hagbarth, "Activity from skin mechanoreceptors recorded percutaneously in awake human subjects," *Expl. Neurol.*, vol. 21, pp. 270–289, 1968.

[37] Å. B. Vallbo and R. S. Johansson, "Properties of cutaneous mechanoreceptors in the human hand related to touch sensation," *Human Neurobiology*, vol. 3, pp. 3–14, 1984.

[38] J. G. Webster, "Artificial sensors suitable for closed-loop control of FNS," in R. B. Stein, H. P. Peckham, and D. Popovic, Eds., *Neural Prostheses: Replacing Motor Function after Disease or Disability.* New York: Oxford Univ. Press, 1992, pp. 88–98.

recordings," in *Proc. Annu. Int. Conf. IEEE Eng. Med. Biol. Soc.*, vol. 13, 1991, pp. 896–897.

[39] G. Westling and R. S. Johansson, "Responses in glabrous skin mechanoreceptors during precision grip in humans," *Exp. Brain Res.*, vol. 66, pp. 128–140, 1987.

[40] W. D. Willis, Jr., and R. E. Coggeshall, *Sensory mechanisms of the spinal cord,* 2nd ed. New York: Plenum Press, 1991.

[41] M. A. Haugland and J. A. Hoffer, "Artifact-free sensory nerve signals obtained from cuff electrodes during functional electrical stimulation of nearby muscles," *IEEE Trans. Rehab. Eng.*, this issue, pp. 000–000.

[42] L. A. Bernotas, P. E. Crago, H. J. Chizeck, M. R. Neuman, and F. T. Hambrecht, "Sensors for use with functional neuromuscular stimulation," *IEEE Trans. Biomed. Eng.*, vol. 33, pp. 256–268, 1986.

[43] A. Iggo and H. Ogawa, "Correlative physiological studies of rapidly adapting mechanoreceptors in cat's glabrous skin," *J. Physiol.*, vol. 266, pp. 275–296, 1977.

[44] W. Jänig, "The afferent innervation of the central pad of the cat's hind foot," *Brain Research*, vol. 28, pp. 203–216, 1971.

[45] R. S. Johansson and Å. B. Vallbo, "Tactile sensibility in the human hand: Relative and absolute densities of four types of mechanoreceptive units in the glabrous skin," *J. Physiol.*, vol. 286, pp. 283–300, 1979.

[46] B. Lynn, "The form and distribution of the receptive fields of pacinian corpuscles found in and around the cat's large foot pad. "*J. Physiol.*, vol. 217, pp. 755–771, 1971.

[47] P. H. Peckham and M. W. Keith, "Motor prostheses for restoration of upper extremity function," in *Neural Prostheses: Replacing Motor Function After Disease or Disability*, (R. B. Stein, H. P. Peckham, and D. Popovic, Eds.). London: Oxford Univ. Press, 1992, pp. 162–187.

J. Andy Hoffer received the B.S. degree in physics from Harvey Mudd College, Claremont, CA, in 1970 and the Ph.D. degree in biophysics from Johns Hopkins University, Baltimore, MD, in 1975.

From 1975 to 1978 he was a Muscular Dystrophy Association post-Doctoral Fellow in the Physiology Department, University of Alberta, Edmonton, Canada. From 1978 to 1982 he was a Senior Staff Fellow at the Laboratory of Neural Control, NINDS, NIH, in Bethesda, MD. In 1982 he was a Visiting Professor at the Institute of Neurophysiology, National Research Center, Milan, Italy. From 1982 to 1991 he was a faculty member at the Departments of Clinical Neurosciences and Medical Physiology, University of Calgary in Alberta, Canada, where he became Professor in 1991. Since 1991 he has been Professor and Director of the School of Kinesiology, Faculty of Applied Sciences, Simon Fraser University, Burnaby, BC, Canada. His present research areas include the neural control of movements, particularly the activity patterns and reflex actions of muscle and skin receptors in voluntary movements, and the development of techniques for recording, processing, and analyzing nerve and muscle activity suitable for controlling neural prostheses.

Dr. Hoffer was awarded an Alberta Heritage Medical Scholarship from 1982 to 1992. He is currently a member of the Biomedical Engineering Grants Committee of the Medical Research Council of Canada. He is a member of the Engineering in Medicine and Biology Society, the Society for Neuroscience, and the International Brain Research Organization.

Thomas Sinkjaer received the M.Sc.E.E. from Aalborg University, Denmark, in 1983, with specialization in biomedical engineering, and the Ph.D. degree in 1988. His dissertation was a joint-venture project between University of Calgary, Canada, and Aalborg University.

From 1984 to 1986, he studied at the Department of Clinical Neurosciences, University of Calgary and during 1989–1990 at the Department of Physiology, Northwestern University, Chicago, IL. Since 1986, he has been with the Department of Medical Informatics and Image Analysis as an Associate Professor. In 1992 he was made Head of the Department and most recently Research Council Professor and Head of the Center for Sensory-Motor Interactions/Neural Prostheses, which was established in 1993 under the Department of Medical Informatics and Image Analysis. His research interests include electrophysiology, biomechanics, motor control (human sensory-motor interaction), and neural prostheses.

He holds a wide number of offices, among them an Expert for the EC (DG XIII) Program Biomed I and a referee for various international journals.

Morten K. Haugland was born in Holstebro, Denmark, on June 1, 1964. He received the M.Sc.E.E. degree in July 1989 and the Ph.D. degree in biomedical engineering in 1994, from Aalborg University, Denmark.

From 1989 to 1990 he worked as a Research Assistant in Dr. J. A. Hoffer's laboratory at the University of Calgary, Canada. He is currently employed as Assistant Professor in the Department of Biomedical Engineering at Aalborg University, Denmark.